Inclusion Compounds

Deutsche Ausgabe: DOI: 10.1002/ange.201500884
Internationale Ausgabe: DOI: 10.1002/anie.201500884

Dynamic Gas-Inclusion in a Single Crystal**

*Satoshi Takamizawa**

Abstract: *In solid-state science, most changing phenomena have been mysterious. Furthermore, the changes in chemical composition should be added to mere physical changes to also cover the chemical changes. Here, the first success in characterizing the nature of gas inclusion in a single crystal is reported. The gas inclusion process has been thoroughly investigated by in situ optical microscopy, single-crystal X-ray diffraction analyses, and gas adsorption measurements. The results demonstrated an inclusion action of a first-order transition behavior induced by a critical concentration on the phase boundary. The transfer of phase boundary and included gas are strongly related. This relationship can generate the dynamic features hidden in the inclusion phenomena, which can lead to the guest capturing and transfer mechanism that can apply to spatiotemporal inclusion applications by using host solids.*

Microporous metal complexes are investigated for applications in gas storage, gas purification, and as catalysts to make use of the superior designability of the pore structures.[1] Single-crystal-to-single-crystal phase transitions induced by gaseous-guest sorption in those metal complexes have received significant attention due to the possibilities of switching the properties of a solid such as emission, electric conductivity, and magnetism.[2] Investigation of the correlation between guest diffusivity and structural transition in microporous crystalline solids began with a quantitative study of guest desorption in Hoffman–type complexes in 1976.[3] In the following years, guest diffusion in host solids involving structural transitions were visually observed and theoretically analyzed[4] but the propagation mechanism of the guest-diffusion-induced transition through a whole single crystal is still unclear. This is due to the inhibition caused by the complicated distribution of inclusion states over the whole crystal and its unsuitable configuration.

My group has developed molecular single-crystal hosts of $[Cu_2(bza)_4(pyz)]_n$ (**1**; bza: benzoate; pyz: pyrazine) and its derivatives which exhibit the apparently conflicting properties of crystal regularity and structural flexibility and can generate gas-inclusion cocrystals with various inorganic gases and organic vapors while preserving the single-state solid morphology.[5] The flexible single-crystal host can surmount the past experimental problems and provide an occasion for the in situ observation of the relationship between micro- and macroscopic change phenomena induced by guest diffusion within the whole crystal.

In previous reports, my group confirmed novel dynamic gas separation behavior in the single-crystal host of **1**, which is capable of adsorbing various gases within its channels.[6] Based on the high stability of **1** to prevent structural defects during gas adsorption, my group has performed a single-crystal X-ray diffraction analysis of gas-inclusion cocrystals even at higher temperature and pressure (up to 100 °C and 42 MPa of gas pressure), which can grasp the detailed structures under equilibrium conditions.[7] Because the gas adsorption profile with a significant leap indicated a kind of transition phenomena related to the gas supply, it is proposed that the "mass-induced phase transition" mechanism,[8] which causes first-order phase transition behavior, is triggered by a critical adsorption amount which allows a two-phase coexistence during the adsorption leap. Considering the high stability of the single crystal of **1** in the gas-inclusion state, the kinetics of the phase-changing behavior can be observed during gas adsorption. By focusing on the moderate speed of EtOH adsorption,[9] we observed the crystal under the controlled pressure of EtOH vapor at 293 K.

Surprisingly, boundary generation was clearly observed in the adsorption process under an optical microscope with a polarizer (movie S1).[10,11] Upon introducing EtOH vapor, different colored areas emerged from all sides of the crystal surfaces [crystal surface of (100); crystal surface of $(\bar{1}11)$] but not from the top surface of the crystal (001), followed by color bleeding (Figure 1 and the Supporting Information, SI). Considering a one-dimensional channel parallel to the crystal surface of (001), these results demonstrate anisotropic gas adsorption of the EtOH vapor into the crystal along this channel. The colored area appeared when 38 mmHg of EtOH vapor was passed, which is the adsorption leap pressure in the adsorption isotherm of **1** (Figure 2). The color change that occurred during the crystal phase transition was confirmed by visible adsorption spectra and explains the linkage between the weak interaction of the physical gas adsorption and the solid-state phase transition that potentially exhibits the so-called "vapochromism" phenomenon (SI).

Since single-crystal X-ray analysis at 293 K[12] showed the crystal phase transition from *C*2/*c* (α phase of the host crystal system) to the *P*-1 space group (β phase), in which the volume increased 8.5% by adsorbing EtOH vapor, the boundary should be assigned as the interface between the two host-crystal phases. This suggests that the EtOH adsorption of **1** induces a first-order phase transition around the phase boundary, which agrees well with Gibbs' phase rule[13] for first-order transitions. Consequently, if the temperature is determined, the gas pressure and the critical amount of gas adsorption will be uniquely determined. It is noteworthy that

[*] Prof. Dr. S. Takamizawa
Graduate School of Nanobioscience, Yokohama City University
Seto 22-2, Kanazawa-ku, Yokohama, 236-0027 (Japan)
E-mail: staka@yokohama-cu.ac.jp

[**] This work was supported in part by the PRESTO program of Japan Science and Technology (JST) and a Grant-in-aid for Fundamental Scientific Research (B) (Grant No. 23350028).

Supporting information for this article is available on the WWW under http://dx.doi.org/10.1002/anie.201500884.

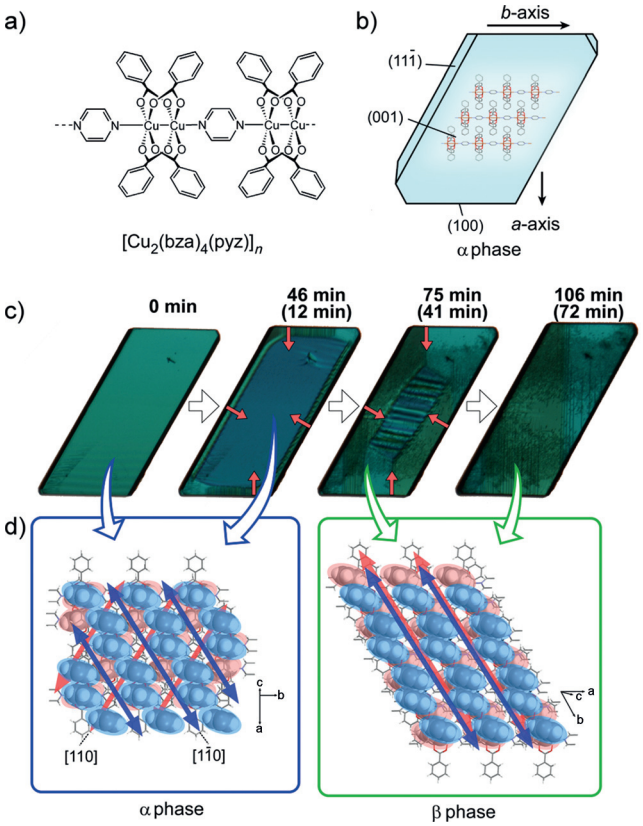

Figure 1. Behavior of phase transition in single crystal of **1** during ethanol adsorption. a) Chemical structure and b) conceptual figure of crystal **1** with the direction of the channel. c) Photographs of the crystal (crystal size: 650 μm × 230 μm) observing the phase transition under controlled pressure of EtOH (first 15 min: 30 mmHg, after 15 min: 40 mmHg); crystal of **1** before EtOH adsorption (left), in the process of phase transition (center), and after the phase transition (right). d) Crystal packing structure of **1** with the direction of the channel at 293 K before phase transition (left: α phase (*C*2/*c*)) and after phase transition (right: β phase (*P*-1)). Included EtOH molecules are omitted for clarity. Times shown in parentheses are from the start of phase transition.

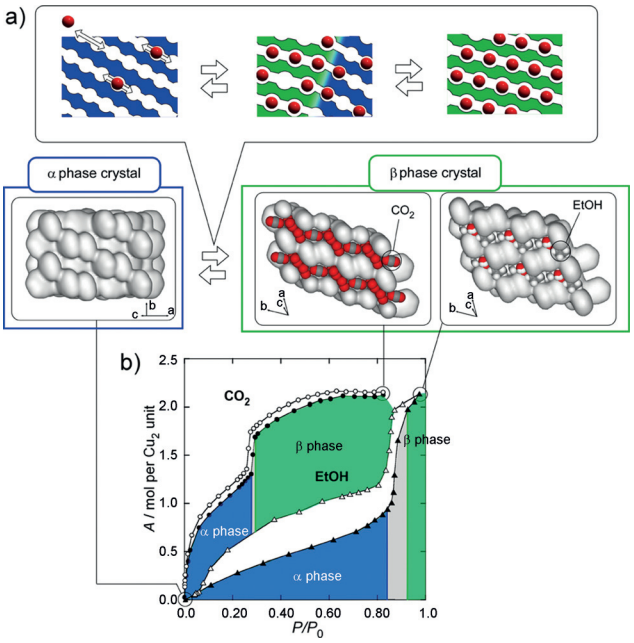

Figure 2. Correlation between crystal phase transition and adsorption leaps for **1**. a) Conceptual images for proceeding of phase transition from α-phase crystal (left image marked with blue frame) to β-phase crystals (two right figures marked with green frame). b) Adsorption isotherm of CO_2 (closed circles) and EtOH (closed triangles) at 293 K on BELSORP-HP (BEL Japan) and Autosorb-1-VP (Quantachrome). Pressure is shown as relative pressure with saturated pressures (P_0) at 5.7 MPa for CO_2 and 44 mmHg (5.9 kPa) for EtOH. The colors indicate the crystal state for α-phase (blue), β-phase (green), and α-β two-phase coexistence during crystal transition (gray).

the phase transition in the crystal cooperatively progresses in keeping the phase boundary surface flat.

Since the boundary emerges from the opening channels on the crystal face, the boundary movement should be correlated to the gas diffusion inside the channels, which is induced by the outside atmosphere. Thus, gas diffusion can be estimated by the boundary movement based on the guest supply to the interface.

The expanding rate of the phase change was estimated from plotting the distance (x) of the interface line from the crystal surface of (100) and ($\bar{1}$11) in the phase transition step (Figure 3). The plot of ln$x$ versus ln$t$ shows a linear relationship in the first half and the second half with the different gradients: 0.5 for the first half and 1.0 for the second half. These gradient values demonstrated the switch of the rate-determining process from gas-diffusion-limited access to phase-transition-limited access.

The gas-diffusion-limited access refers to the gas-diffusion behavior in crystals. Although the apparent velocities of the phase boundary movement were different from the (100) and ($\bar{1}$11) surfaces, both turned out to be the same velocity along the channel directions by considering the channel-penetrating angle from each crystal surface and the gas concentration by volume. This shows that the guest molecules diffuse along the channel in the same manner independent of the crystal surfaces.

Although the gas concentration must form a gradient from the crystal surface to deep inside, the first-order transition behavior requires that the constant concentrations should be maintained on both sides of the interface (Figure 3b). In a precise sense, a strict two-phase equilibrium is only present directly at the interface, which allows the apparent first-order transition in the sense of gas adsorption. This is considered to be the essential meaning of the change in the adsorption-induction phase (mass-induced phase transition)[8] which makes the critical adsorption mass a trigger to generate and transfer the phase boundary. By using the critical amounts at both ends of the adsorption leap from the adsorption isotherm curve, calculation of the diffusion coefficient was based on the movement of the contour line of the concentration of included gas.[14]

The elucidated diffusion coefficients in the β-phase channel are 10^{-10} $m^2 s^{-1}$ derived from the behavior of the boundary movement, which is larger by four orders of magnitude than that in zeolite (10^{-14} $m^2 s^{-1}$) and is close to the Knudsen diffusion on activated carbon,[15] thereby dem-

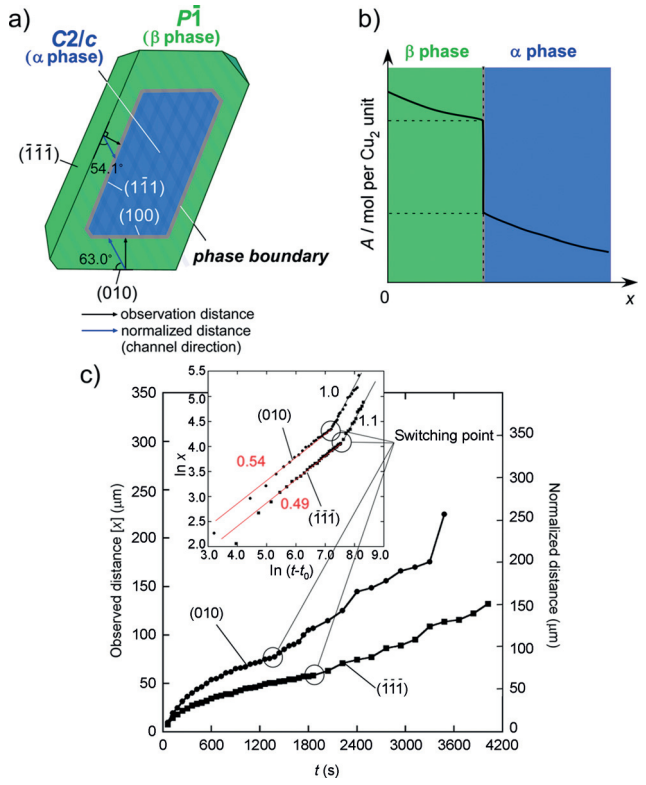

Figure 3. Time course of phase propagation. a) Geometry of phase boundary in single crystal of **1** and b) discontinuity in the guest concentration across the phase boundary. c) Plot of distance (x) versus time (t) from the beginning of the phase transition. Inset: Plot of ln$x$ versus ln$t$ (gradient: 0.49 and 1.1 for ($\bar{1}11$); 0.54 and 1.0 for (100)).

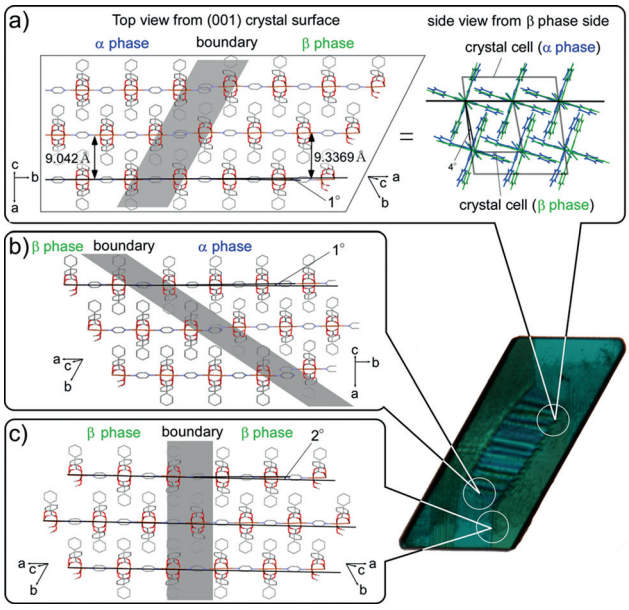

Figure 4. Predictable structure at each boundary from top view (a–c) and side view (inset of a). a,b) The α-β phase boundary and c) β-β phase boundary. As shown in the side view structure of the α-β phase boundary, the α-phase crystal structure (blue) and β-phase crystal structure (green) mismatch at the phase boundary. The angles shown in the figure are the bending angle of the 1D chain under the assumption that the crystal surfaces at the phase boundary were firmly bonded. (Distance and angle strains are required in the α-β interface (a, b), whereas only bending is required in the β-β twin interface (c).)

onstrating the fast gas diffusion inside a channel (SI). The value in the α-phase channel, which is given by the movement of the color bleeding before transition, is almost the same as in the β-phase channels, indicating that fast diffusion occurs inside both channels in α- and β-phase crystals. CO_2 gas also has a large diffusion coefficient of 10^{-7} m^2s^{-1}, which is seven orders of magnitude larger than those in zeolites (10^{-14}–10^{-15} m^2s^{-1}; SI). This result suggests smooth guest transfer inside the channels of **1** and the distinct acceleration in diffusing the smaller guest CO_2 agrees with the space-expansion effect through local expansion of channel portions reported previously.[6c] Considering the coexistence of two crystal phases as a single solid, defects in crystal packing and/or distortion of the host molecular structure is expected depending on the incompatibility of the joint area between the different crystal phases. Superposition of the X-ray crystal structures on the bonded surfaces indicated the strain of the one-dimensional chain complex (Figure 4). Although the changes of width and angle require unconformity of the interface stratum, the experimental results did not reveal any breaking crystal, suggesting that the one-dimensional (1D) coordination complex chain was flexible enough to withstand the strain. The appearance of a flat interface indicates that the structurally inconsistent points on the 1D skeletons tend to be aligned to effectively minimize the distortion energy in the entire crystal and any crystal-packing distortion. In this picture, the interface can easily move while maintaining crystal integrity, because the mere movement of the well-organized strain stratum formed by the distorted points on the 1D host skeleton can advance the crystal transition without a large strain on the crystal.

In conclusion, the dynamic inclusion process was clearly characterized in situ. The results elucidated the characteristics of dynamic gas inclusion driven by the spatiotemporal distribution of guest, microscopic structure, and macroscopic phase in a single solid. The discovered fundamentals of dynamic inclusion action will contribute not only to pure inclusion chemistry but also lead to mechanism principles for next-generation inclusive applications such as spatiotemporal guest transfer under dynamic control of guest supply, movement, and discharge processes through cooperative micro- and macroscopic structural changes coupled by guest inclusion.

Keywords: coordination compounds · crystals · diffusion · inclusion compounds · phase transitions

How to cite: *Angew. Chem. Int. Ed.* **2015**, *54*, 7033–7036
Angew. Chem. **2015**, *127*, 7139–7142

[1] a) J. Y. Lee, O. K. Farha, J. Roberts, K. A. Scheidt, S. T. Nguyen, J. T. Hupp, *Chem. Soc. Rev.* **2009**, *38*, 1450–1459; b) Y. H. Hu, L. Zhang, *Adv. Mater.* **2010**, *22*, E117–E130; c) S. Noro, *Phys. Chem. Chem. Phys.* **2010**, *12*, 2519–2531; d) M. Shah, M. C.

McCarthy, S. Sachdeva, A. K. Lee, H. K. Jeong, *Ind. Eng. Chem. Res.* **2012**, *51*, 2179 – 2199; e) V. Guillerm, D. Kim, J. F. Eubank, R. Luebke, X. Liu, K. Adil, M. S. Lah, M. Eddaoudi, *Chem. Soc. Rev.* **2014**, *43*, 6141 – 6172; f) H. Sato, W. Kosaka, R. Matsuda, A. Hori, Y. Hijikata, R. V. Belosludov, S. Sakaki, M. Takata, S. Kitagawa, *Science* **2014**, *343*, 167 – 170.

[2] a) G. J. Halder, C. J. Kepert, B. Moubaraki, K. S. Murray, J. D. Cashion, *Science* **2002**, *298*, 1762 – 1765; b) P. P. Mazzeo, L. Maini, D. Braga, G. Valenti, F. Paolucci, M. Marcaccio, A. Barbieri, B. Ventura, *Eur. J. Inorg. Chem.* **2013**, 4459 – 4465; c) A. A. Talin, A. Centrone, A. C. Ford, M. E. Foster, V. Stavila, P. Haney, R. A. Kinney, V. Szalai, F. El Gabaly, H. P. Yoon, F. Léonard, M. D. Allendorf, *Science* **2014**, *343*, 66 – 69.

[3] a) M. Sitarski, J. Lipkowski, *Rocz. Chem.* **1976**, *50*, 1129 – 1136.

[4] a) J. E. Lewis, Jr., G. R. Gavalas, M. E. Davis, *AIChE J.* **1997**, *43*, 83 – 90; b) P. V. Kortunov, L. Heinke, M. Arnold, Y. Nedellec, D. J. Jones, J. Caro, J. Kärger, *J. Am. Chem. Soc.* **2007**, *129*, 8041 – 8047; c) T. Haneda, M. Kawano, T. Kawamichi, M. Fujita, *J. Am. Chem. Soc.* **2008**, *130*, 1578 – 1579; d) H. Aggarwal, P. M. Bhatt, C. X. Bezuidenhout, L. J. Barbour, *J. Am. Chem. Soc.* **2014**, *136*, 3776 – 3779.

[5] a) S. Takamizawa, C. Kachi-Terajima, M. Kohbara, T. Akatsuka, T. Jin, *Chem. Asian J.* **2007**, *2*, 837 – 848; b) S. Takamizawa, E. Nakata, T. Akatsuka, R. Miyake, Y. Kakizaki, H. Takeuchi, G. Maruta, S. Takeda, *J. Am. Chem. Soc.* **2010**, *132*, 3783 – 3792.

[6] a) S. Takamizawa, M. Kohbara, R. Miyake, *Chem. Asian J.* **2009**, *4*, 530 – 539; b) S. Takamizawa, Y. Takasaki, R. Miyake, *J. Am. Chem. Soc.* **2010**, *132*, 2862 – 2863; c) Y. Takasaki, S. Takamizawa, *J. Am. Chem. Soc.* **2014**, *136*, 6806 – 6809.

[7] a) S. Takamizawa, Y. Takasaki, R. Miyake, *Chem. Commun.* **2009**, 6625 – 6627; b) S. Takamizawa, E. Nakata, R. Miyake, *Dalton Trans.* **2009**, 1752 – 1760.

[8] S. Takamizawa, T. Saito, T. Akatsuka, E. Nakata, *Inorg. Chem.* **2005**, *44*, 1421 – 1424.

[9] The elucidated process is essentially the same for CO_2 but too fast for accurate analysis. See SI.

[10] In situ observation was performed with a basic optical microscope (NIKON SMZ1500) with a polarizer and analyzer staggered by 40° to observe both α- and β-crystal phases during transition inside a chamber under controlled temperature and gas pressure.

[11] The topological correlation between the direction of the polymeric chain component and the crystal shape was determined for an empty single crystal of $[Cu^{II}_2(bza)_4(pyz)]_n$ (**1**)(*C*2/*c* space group). As shown in Figure 1, the single crystal has a 1D penetration pore crystal in which the channels are gathered in the same direction. The channels in alternate layers are parallel to [110] and those in the other layers are parallel to $[1\bar{1}0]$.

[12] Single-crystal X-ray structural analysis of **1** was performed at 90 K on a Bruker Smart APEX CCD area diffractometer (Bruker AXS). Crystal data of **1** for the empty α phase at 293 K: Monoclinic, C_2/c, $a = 18.083$ (2) Å, $b = 9.7100$ (12) Å, $c = 19.005$ (3) Å, $\beta = 97.327$ (3), $V = 3309.8$ (7) Å^3, $Z = 4$, $D_{calc} = 1.388$ Mg m^{-3}, $R_1 = 0.0446$ (0.0712), $wR_2 = 0.1193$ (0.1321) for 2710 reflections with $I > 2\sigma(I)$ (for 4099 reflections (12081 total measured)), goodness-of-fit on $F^2 = 1.041$, largest diff. peak (hole) = 0.480 (−0.424) e Å^{-3}. The β phase including ethanol vapor at 293 K: Triclinic, *P*-1, $a = 9.746$ (2) Å, $b = 10.483$ (2) Å, $c = 11.095$ (3) Å, $\alpha = 69.564$ (4)°, $\beta = 65.092$ (4)°, $\gamma = 62.958$ (4)°, $V = 898.1$ (4) Å^3, $Z = 1$, $D_{calc} = 1.415$ Mg m^{-3}, $R_1 = 0.0553$ (0.0704), $wR_2 = 0.1444$ (0.1534) for 2884 reflections with $I > 2\sigma(I)$ (for 3628 reflections (5621 total measured)), goodness-of-fit on $F^2 = 1.111$, largest diff. peak (hole) = 0.943 (−0.358) e Å^{-3}. CCDC 1046311, 1046312 contain the supplementary crystallographic data for this paper. These data can be obtained free of charge from The Cambridge Crystallographic Data Centre via www.ccdc.cam.ac.uk/data_request/cif.

[13] At the state of phase transition, the pressure did not change at constant temperature. This fact obeys Gibbs' phase rule: $F = C - P + 2$, in which *F*, *C*, and *P* are degree of freedom, number of components, and number of phases, respectively. Since the equation can be set to $C = 2$ (gas and host crystal) and $P = 3$ (gas, α-phase and β-phase crystals), the degree of freedom becomes $F = 1$.

[14] By plotting the logarithm of *x* versus that of *t*, the order of time (*t*) that is perpendicular to the distance (*x*) can be estimated by the gradient of the plot. If $x = Ct^n$, in which C is a proportional constant and *t* is time from the start of the phase transition, *n* can be estimated from the gradient of the plot of ln*x* versus ln*t* (i.e., $\ln x = n \ln t + \ln C$: ln*C* is a constant; see SI for details of mathematical handling).

[15] a) D. Bobok, E. Besebová, *Chem. Pap.* **2003**, *57*, 39 – 44; b) B. Sakintuna, E. Fakioglu, Y. Yürüm, *Energy Fuels* **2005**, *19*, 2219 – 2224.

Received: January 30, 2015
Revised: April 2, 2015
Published online: April 29, 2015

